Pramana – J. Phys. (2017) 88: 17
DOI 10.1007/s12043-016-1321-8

Dynamical behaviours and exact travelling wave solutions of modified generalized Vakhnenko equation

JUNJUN XIAO[1,*], DAHE FENG[1,2], XIA MENG[1] and YUANQUAN CHENG[1]

[1]School of Mathematics and Computing Science, Guilin University of Electronic Technology, Guilin, Guangxi 541004, People's Republic of China
[2]School of Mathematics and Statistics, Guizhou University of Finance and Economics, Guiyang, Guizhou 550025, People's Republic of China
*Corresponding author. E-mail: xiaojunjun2013@hotmail.com

MS received 12 May 2015; revised 24 May 2016; accepted 17 June 2016; published online 13 December 2016

Abstract. By using the bifurcation theory of planar dynamical systems and the qualitative theory of differential equations, we studied the dynamical behaviours and exact travelling wave solutions of the modified generalized Vakhnenko equation (mGVE). As a result, we obtained all possible bifurcation parametric sets and many explicit formulas of smooth and non-smooth travelling waves such as cusped solitons, loop solitons, periodic cusp waves, pseudopeakon solitons, smooth periodic waves and smooth solitons. Moreover, we provided some numerical simulations of these solutions.

Keywords. Modified generalized Vakhnenko equation; cusped solitons; loop solitons; periodic cusp wave solutions; smooth periodic wave solutions; pseudopeakon solitons; smooth soliton solutions.

PACS Nos 05.45.Yv; 02.30.Jr; 02.30.Oz

1. Introduction

In 1992, Vakhnenko [1] constructed the following Vakhnenko equation (VE):

$$\frac{\partial}{\partial x}\left(\frac{\partial}{\partial t}+u\frac{\partial}{\partial x}\right)u+u=0,$$

to describe high-frequency waves in a relaxing medium, and derived two families of periodic travelling wave solutions to the VE corresponding to the propagation in the positive and negative x directions respectively. In 1993, Parkes [2] showed both families of solutions given by Vakhnenko were stable under long wavelength perturbations of small amplitude. A remarkable feature of the VE is that it has a loop soliton expressed by a multivalued function [3]. Moreover, Vakhnenko and Parkes obtained the two-loop soliton solution and the multiloop soliton solution to the VE by using both Hirota's method [4] and inverse scattering transform (IST) [5]. Wu *et al* [6] applied the homotopy analysis method and derived a one-loop soliton solution to the VE expressed by a series of exponential functions. Recently, Ma and Li [7] discussed the non-travelling wave solutions to the VE by using the (G_0/G)-expansion method and gained many interesting periodic solutions and solitary solutions.

In 2003, Vakhnenko *et al* [8] presented a generalization of the VE, namely (GVE)

$$\frac{\partial}{\partial x}\left(D^2u+\frac{1}{2}u^2+\beta u\right)+Du=0,\ D:=\frac{\partial}{\partial t}+u\frac{\partial}{\partial x},$$

and derived the N-soliton solution of the GVE and other different types of solitons such as loops, humps and cusps.

Meanwhile, Morrison and Parkes [9] first introduced the modified generalized Vakhnenko equation (mGVE)

$$\frac{\partial}{\partial x}\left(D^2u+\frac{1}{2}pu^2+\beta u\right)+qDu=0,\quad D:=\frac{\partial}{\partial t}+u\frac{\partial}{\partial x},\tag{1}$$

where p, q and β are arbitrary non-zero constants, and gained some N-soliton solutions to the mGVE using a blend of transformations of the independent variables and Hirota's method. Obviously, the VE can be obtained from the mGVE if $p=q=1$ and $\beta=0$, while the GVE corresponds to $p=q=1$ and β an arbitrary non-zero constant. Ma and Li constructed a series of smooth travelling wave solutions to the mGVE using the auxiliary equation method [10] and a

variable transformation method [11]. Wazwaz [12] derived several multiple soliton solutions for the mGVE using a simplified Hirota's bilinear method. Hashemi *et al* [13] applied the Lie symmetry group preserving scheme and determined the Lie point symmetry algebra, and corresponding similarity reductions of the mGVE.

Obviously, the mGVE (1) has a strong nonlinear structure. It is very difficult to analyse its general solutions because of the complexity of nonlinearity, and so it is very important to do the qualitative analysis of the solutions. Here we concentrate on the travelling wave solutions to the mGVE (1) under consideration. By using the bifurcation theory of planar dynamical systems and the qualitative analysis of differential equations [14–18], we discuss the dynamical behaviours and the bifurcations of the travelling waves of eq. (1) and derive a series of abundant travelling wave solutions including cusped solitons, loop solitons, periodic cusp waves, pseudopeakon solitons, smooth periodic waves and smooth solitons.

In order to obtain the exact solution for the mGVE (1), we introduce a travelling wave transformation

$$u = u(\xi), \quad \xi = x - ct, \tag{2}$$

where $c > 0$ is the wave speed. Substituting (2) into eq. (1) and integrating once, we get the following ordinary differential equation (ODE):

$$(u-c)^2u''+(u-c)u'^2+\frac{p+q}{2}u^2+(\beta-cq)u = g, \tag{3}$$

where $u' = \mathrm{d}u/\mathrm{d}\xi$ and g is a constant of integration.

Making the transformation $u = u - c$, eq. (3) becomes

$$u^2u'' + uu'^2 + Mu^2 + Nu + G = 0, \tag{4}$$

where

$$M = \frac{p+q}{2}, \quad N = cp + \beta$$

and

$$G = \frac{p-q}{2}c^2 + c\beta - g.$$

Clearly, eq. (4) is equivalent to the planar Hamiltonian system

$$\frac{\mathrm{d}u}{\mathrm{d}\xi} = y, \quad \frac{\mathrm{d}y}{\mathrm{d}\xi} = -\frac{uy^2 + Mu^2 + Nu + G}{u^2} \tag{5}$$

with the Hamiltonian function

$$H(u, y) = \frac{1}{2}u^2y^2 + \frac{1}{3}Mu^3 + \frac{1}{2}Nu^2 + Gu = h, \tag{6}$$

where h is the Hamiltonian constant.

Equation (5) is a three-parameter planar dynamical system depending on the parameters M, N and G. Because the phase orbits defined by the vector field of (6) determine all travelling wave solutions of (5), we should investigate the bifurcations of phase portraits of eq. (5) in the (u, y)-phase plane as the parameters M, N and G change.

From the theory of dynamical systems [14], the classical analytic travelling wave solutions of eq. (1) are given by classical analytic orbits of the dynamical system (5): a solitary wave solution corresponds to a homoclinic orbit at a single equilibrium point; a periodic wave comes from a periodic orbit; while a heteroclinic orbit connecting two equilibrium points yields analytic kink solutions. Thus, to investigate the bifurcations of solitary waves, kink waves and periodic waves of eq. (1), we shall find all periodic annuli, homoclinic and heteroclinic orbits of (5) depending on the parameter space of the systems. The bifurcation theory of dynamical system [14] plays a key role in our study.

But we notice particularly that the right-hand side of the second equation in (5) is discontinuous when $u = 0$. In other words, $u_{\xi\xi}$ has no definition on the straight line $u = 0$ in the (u, y)-phase plane. We call $u = 0$ the singular line leading to the non-analytic dynamical behaviour and present that the existence of a singular point is the original reason for the appearance of non-smooth solutions. Here we consider the dynamical behaviours and bifurcations of (5) with the singular line $u = 0$ and call eq. (5) the singular system. According to the bifurcation sets and the corresponding phase portraits, we obtain many smooth and non-smooth travelling wave solutions of the mGVE (1).

In this paper, we only consider the case when $M > 0$ because of the invariance of eq. (5) under the transformation $M \to -M, u \to -u, y \to -y$.

The rest of the paper is organized as follows. In §2 and 3, we discuss the bifurcations and phase portraits of eq. (5) for $G = 0$ and $G \neq 0$ respectively and construct a series of abundant exact travelling wave solutions of eq. (1). A conclusion is then given in §4.

2. Bifurcations and exact travelling wave solutions of eq. (5) when $G = 0$

In this section, we shall study all possible bifurcations and phase portraits of the vector fields defined by eq. (5) when $G = 0$ in the parametric space and find the exact travelling wave solutions of eq. (1).

2.1 *Bifurcations of the phase portraits of eq.* (5) *when* $G = 0$

Because of the difficulty to directly study the singular system (5), we make the time-scale transformation $\mathrm{d}\xi = u\,\mathrm{d}\eta$ and reduce the singular system (5) with $G = 0$ to the regular system

$$\frac{\mathrm{d}u}{\mathrm{d}\eta} = uy, \quad \frac{\mathrm{d}y}{\mathrm{d}\eta} = -y^2 - Mu - N \tag{7}$$

with the corresponding Hamiltonian function

$$H(u, y) = \frac{1}{2}u^2y^2 + \frac{1}{3}Mu^3 + \frac{1}{2}Nu^2 = h \tag{8}$$

which can be reduced from eq. (6) if $G = 0$.

Obviously, eq. (7) has the same topological phase portraits as eq. (5) with $G = 0$ except on the singular line $u = 0$. Both eqs (7) and (5) are integrable and have the same first integral as eq. (8). For a fixed h, eq. (8) determines a set of invariant curves of eq. (7), containing different branches of curves. As h is varied, eq. (8) defines different families of orbits of eq. (7) with different dynamical behaviours.

Clearly, for $N \geq 0$, eq. (7) has a unique equilibrium point at $P_1(-N/M, 0)$. As $N < 0$, there are three equilibrium points of (7) at P_1, $P_2(0, \sqrt{-N})$ and $P_3(0, -\sqrt{-N})$. Let (u_e, y_e) be any equilibrium point of (7) and $J(u_e, y_e)$ be the determinant of the coefficient matrix for the linearized system of (7) about this point. Thus, we have

$$J(-N/M, 0) = -N, \quad J(0, \pm\sqrt{-N}) = 2N. \tag{9}$$

By the theory of planar dynamical systems, we know that as a simple equilibrium point of a planar integrable system, (u_e, y_e) is a saddle (centre) if $J < 0\,(>0)$; it is a cusp if $J = 0$ and its Poincaré index is zero. Thus P_1 is a saddle (centre) for $N > 0\,(<0)$ and a higher equilibrium point for $N = 0$, while both P_2 and P_3 are saddles.

By using the above information and with the aid of *Maple*, we obtain the phase portraits of (7) shown in figure 1.

2.2 *Exact travelling wave solutions of eq.* (5) *when* $G = 0$

In this subsection we discuss the exact travelling wave solutions of the mGVE (1). Let

$$h_1 = H(-N/M, 0) = \frac{N^3}{6M^2},$$
$$h_2 = H(0, \pm\sqrt{-N}) = 0. \tag{10}$$

We notice that the singular system (5) has the same orbits as the regular system (7) except on the singular line $u = 0$. Transformation of variables $\mathrm{d}\xi = u\,\mathrm{d}\eta$ only derives the difference between the parametric representations of orbits of (5) and the counterparts of (7) when $u \neq 0$. It means that in the (u, y)-plane the profiles defined by the orbits of (5) far from the singular line $u = 0$ are smooth. Then we study the dynamical property of the orbits which are close to the singular line or intersect the singular line at other points except for the origin O. We take the case in figure 1c for example. For other cases, we have similar results. From figure 1c, we find that for $h \in (h_1, 0)$, there is one family of periodic orbits Γ^h on the right half (u, y) plane which intersect the u-axis at $(u_1^h, 0)$ and $(u_2^h, 0)$ $(0 < u_1^h < u_2^h)$. It is obvious that $u_1^h \to 0^+$ as $h \to 0^-$. Hence let $u = \epsilon\,(0 < \epsilon \ll 1)$, then in the small right neighbourhood of the singular axis

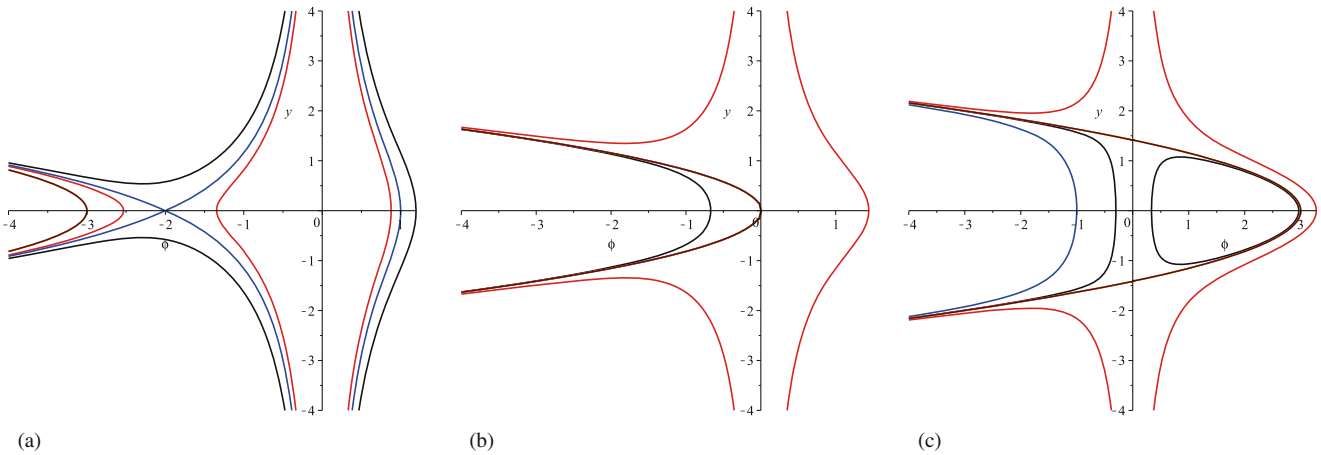

Figure 1. The phase portraits of eq. (5) for $M > 0$, $G = 0$ when (**a**) $N > 0$, (**b**) $N = 0$ and (**c**) $N < 0$.

$u = 0$, (5) gives the following relaxation oscillation form:

$$\frac{\mathrm{d}u}{\mathrm{d}\xi} = y, \quad \epsilon\frac{\mathrm{d}y}{\mathrm{d}\xi} = -y^2 - M\epsilon - N. \tag{11}$$

Thus, for the periodic orbit Γ^h, we introduce the following two lemmas [17]:

Lemma 1. [*The rapid-jump property of the derivative near the singular straight line*]. *Suppose that there exists a family of periodic orbits in the right (or left) neighbourhood of a singular straight line. Then, along a segment of every orbit near the straight line, the derivative of the wave function jumps down (or up) rapidly in a very short time interval.*

Lemma 2. [*Existence of finite time interval of solution with respect to the wave variable in the positive or negative direction*]. *For a singular nonlinear travelling wave system, if an orbit transversely intersects with a singular straight line at a point or approaches a singular straight line, but the derivative tends to infinity, then it only takes a finite time interval to make the moved point of the orbit arrive on the singular straight line.*

It follows from Lemma 1 that if a phase point (u, y) moves near the singular line $u = 0$ along the periodic orbit Γ^h, $y = u_\xi$ changes its sign rapidly from '$-$' to '$+$' which forms a profile of the cusp wave. The existence of the straight line $u = 0$ on the (u, y)-plane of eq. (5) results in the appearance of non-smooth travelling wave solutions such as cusped soliton solutions, loop soliton solutions and periodic cusp wave solutions. Now we consider the exact smooth and non-smooth travelling waves of eq. (5).

2.2.1 *Cusped soliton solution*. For $N > 0$, corresponding to $H(u, y) = h_1$ defined by eq. (8), eq. (5) has two stable manifolds and two unstable manifolds starting from the saddle P_1 (see figure 1a). When $h = h_1$, it follows from eq. (8) that

$$H(u, y) = \frac{1}{2}u^2y^2 + \frac{1}{3}Mu^3 + \frac{1}{2}Nu^2 = h_1 = \frac{N^3}{6M^2}. \tag{12}$$

Then,

$$y = \pm\frac{\sqrt{6M(\phi_2 - u)}}{3u}(u - \phi_1), \tag{13}$$

where

$$\phi_1 = -\frac{N}{M}, \quad \phi_2 = \frac{N}{2M}.$$

Substituting eq. (13) into the first equation of system (5) yields

$$\frac{u\,\mathrm{d}u}{(u - \phi_1)\sqrt{\phi_2 - u}} = \pm\sqrt{\frac{2M}{3}}\,\mathrm{d}\xi. \tag{14}$$

Integrating it along the orbit with the initial value $u(0) = 0$, one can get

$$\int_0^u \frac{u\,\mathrm{d}u}{(u - \phi_1)\sqrt{\phi_2 - u}} = \pm\int_0^\xi \sqrt{\frac{2M}{3}}\,\mathrm{d}\xi. \tag{15}$$

Then we have

$$-\sqrt{\frac{2N}{M} - 4u} + \sqrt{\frac{8N}{3M}}\tanh^{-1}\left(\sqrt{\frac{N - 2Mu}{3N}}\right) - \mu_1 = \pm\sqrt{\frac{2M}{3}}\xi, \tag{16}$$

where

$$\mu_1 = -\sqrt{\frac{2N}{M}} + \sqrt{\frac{8N}{3M}}\tanh^{-1}\left(\frac{\sqrt{3}}{3}\right).$$

By introducing a new parametric variable χ where

$$\chi = \tanh^{-1}\left(\sqrt{\frac{N - 2Mu}{3N}}\right), \tag{17}$$

one can obtain the following parametric representation of u:

$$u(\chi) = \frac{N}{2M}(1 - 3\tanh^2(\chi)). \tag{18}$$

Substituting eq. (18) into (16) leads to the parametric representation of ξ

$$\xi(\chi) = \pm\frac{\sqrt{N}}{M}(2\chi - 3\tanh(\chi) + \sqrt{3} - 2\tanh^{-1}(\sqrt{3}/3)). \tag{19}$$

Thus, one can derive the parametric representation of cusped soliton solution of eq. (5)

$$\begin{cases} u(\chi) = \dfrac{N}{2M}(1 - 3\tanh^2(\chi)), \\ \xi(\chi) = \pm\dfrac{\sqrt{N}}{M}(2\chi - 3\tanh(\chi) + \sqrt{3} - 2\tanh^{-1}(\sqrt{3}/3)), \end{cases} \tag{20}$$

where the value $\chi \in [\tanh^{-1}(\sqrt{3}/3), +\infty)$ plays the role of the parameter in these dependence. The profile of the cusped soliton solution (20) is shown in figure 2a.

2.2.2 *Loop soliton solution*. When $N > 0$, similar to §2.2.1, integrating eq. (14) with the initial value

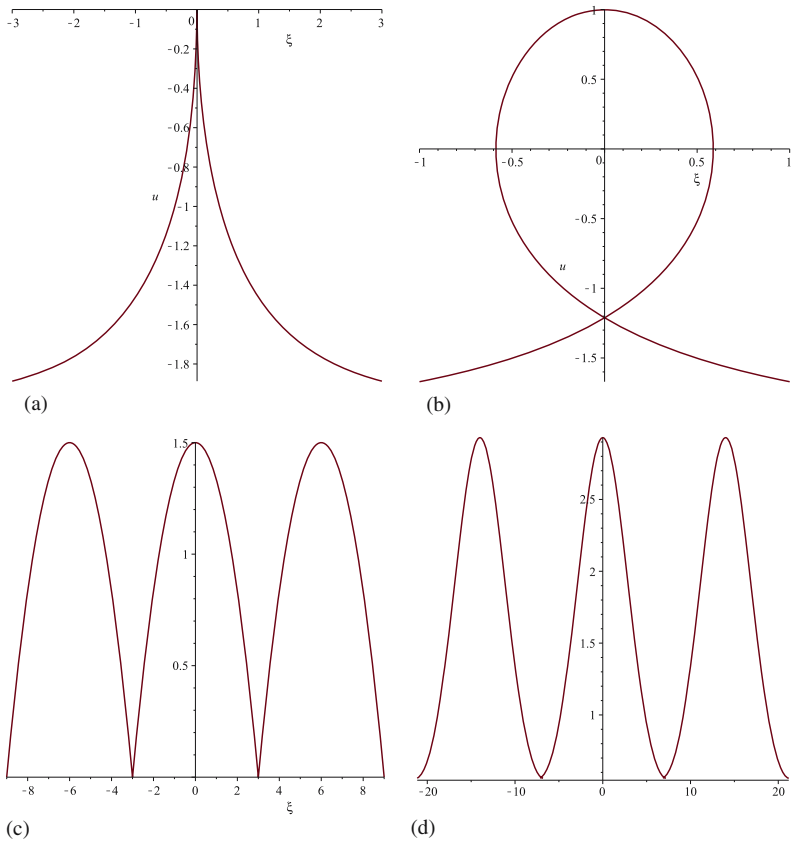

Figure 2. The wave profiles of the solutions $u(\xi)$ with different types. (**a**) Cusped soliton, (**b**) loop-soliton, (**c**) periodic cusp wave and (**d**) smooth periodic wave.

$u(0) = N/2M$, one obtain the following parametric representation of the loop soliton solution of eq. (5):

$$\begin{cases} u(\chi) = \dfrac{N}{2M}\,(1 - 3\tanh^2(\chi)), \\ \xi(\chi) = \dfrac{\sqrt{N}}{M}\,(2\chi - 3\tanh(\chi)), \end{cases} \tag{21}$$

where $\chi \in [-\infty, +\infty)$. The plot of the loop soliton solution (21) is shown in figure 2b.

2.2.3 *Periodic cusp wave solution.* For $N < 0$, as $H(u, y) = h_2 = 0$ defined by eq. (8), there exists an orbit transversely intersecting with the singular line $u = 0$ at the two saddles P_2 and P_3 (see figure 1c), which corresponds to the periodic cusp wave solution of eq. (5). It follows from $H(u, y) = 0$ that

$$y = \pm\frac{1}{\sqrt{3}}\sqrt{2Mu + 3N}. \tag{22}$$

Substituting eq. (22) into the first equation of system (5) and integrating it along the orbit with the initial value $u(0) = -3N/2M$, one can give the parametric representation of the periodic cusp wave solution of system (5)

$$u(\xi) = -\frac{M\xi^2}{6} - \frac{3N}{2M}, \quad \xi \in [-T/2,\ T/2], \tag{23}$$

whose period $T = (6/M)\sqrt{-N}$. The graph of the periodic cusp wave solution (23) is shown in figure 2c.

2.2.4 *Smooth periodic wave solutions.* Suppose that $N < 0$, corresponding to figure 1c, when $h \in (h_1, 0)$, eq. (5) has a family of smooth periodic orbits enclosing the centre P_1. From $H(u, y) = h$ defined by eq. (8), one can get

$$y^2 = \frac{2M}{3u^2}\,(u - r_1)(u - r_2)(r_3 - u), \tag{24}$$

where r_1, r_2, r_3 ($r_1 < r_2 < r_3$) are three real roots of equation $2Mu^3 + 3Nu^2 - 6h = 0$. Substituting eq. (24) into the first equation of system (5) and integrating it along the orbits with the initial value $u(0) = r_3$, we obtain the following parametric representation of smooth periodic travelling wave solutions:

$$\begin{cases} u(\chi) = r_3 - (r_3 - r_2)\,\mathrm{sn}^2(\chi, k), \\ \xi(\chi) = \sqrt{\dfrac{6r_1^2}{M(r_3 - r_1)}}\;\chi + \sqrt{\dfrac{6(r_3 - r_1)}{M}} \\ \qquad \times E(\arcsin(\mathrm{sn}(\chi, k)), k), \end{cases} \tag{25}$$

where $k^2 = (r_3 - r_2)/(r_3 - r_1)$, $\chi \in \mathbb{R}$, $E(\varphi, k)$ is the elliptic integral of second kind and $\mathrm{sn}(u, k)$ is the Jacobian elliptic function with the modulus k [19]. The plot of the smooth periodic travelling wave solution (25) is shown in figure 2d.

Remark 1. Both the cusped soliton solution and loop-soliton solution are singular and non-smooth solitary wave solutions. Moreover, the loop-soliton solution possesses infinite derivatives at certain points.

Remark 2. The arch curve in figure 1c can be treated as the limit curve of the periodic orbits of (5). The periodic cusp wave (23) corresponds to the arch curve, while the smooth periodic waves (25) are derived from the periodic orbits. On the other hand, as h varies from h_1 to zero, $r_3 \to -3N/2M$, $r_{1,2} \to 0$, $k \to 1$. Therefore, $\mathrm{sn}(\chi, k) \to \tanh(\chi)$ and $E(\arcsin(\mathrm{sn}(\chi, k)), k) \to \tanh(\chi)$. It is easy to see from (25) that $u(\chi) \to r_3 - r_3 \tanh^2(\chi)$, $\xi(\chi) \to \sqrt{(6r_3/M)}\tanh(\chi)$ which agrees well with (23). In other words, the smooth periodic waves (25) will gradually lose their smoothness from smooth periodic waves to periodic cusp waves and finally approach periodic cusp wave (23) as $h \to 0^-$.

3. Bifurcations and exact travelling wave solutions of eq. (5) when $G \neq 0$

In this section, we shall study all the possible bifurcations and phase portraits of the vector fields defined by eq. (5) when $G \neq 0$ in the parametric space and find the exact travelling wave solutions of eq. (1).

3.1 *Bifurcations of the phase portraits of eq.* (5) *when* $G \neq 0$

Similar to §2, eq. (5) with $G \neq 0$ is also a singular system. In order to remove the singularity, we introduce the time-scale transformation $\mathrm{d}\xi = u^2\,\mathrm{d}\tau$ and reduce (5) to the regular system

$$\frac{\mathrm{d}u}{\mathrm{d}\tau} = u^2 y, \quad \frac{\mathrm{d}y}{\mathrm{d}\tau} = -(uy^2 + Mu^2 + Nu + G), \quad (26)$$

which has the same topological phase portraits as eq. (5) except on the singular line $u = 0$ and has the same Hamiltonian function as (6).

Now, we investigate the bifurcations of phase portraits of (26). Obviously, all the equilibrium points lie on the u-axes in the (u, y)-phase plane and the horizontal coordinates of the equilibrium points are the real roots of $f(u) = Mu^2 + Nu + G = 0$. There are two equilibrium points at $Q_1(u_1, 0)$ and $Q_2(u_2, 0)$, where $u_{1,2} = (N \pm \sqrt{\Delta})/-2M$ for $\Delta = N^2 - 4MG > 0$. There is a unique equilibrium at $Q_3(u_3, 0)$ where $u_3 = -N/2M$ for $\Delta = 0$ and no equilibrium for $\Delta < 0$. Let $(u_e, 0)$ be an equilibrium point of (26) and $J(u_e, 0)$ be the determinant of the coefficient matrix for the linearized system of (26) about $(u_e, 0)$. Thus, we have

$$J(u_e, 0) = 2Mu_e^2\left(u + \frac{N}{2M}\right). \quad (27)$$

Therefore, $J(u_1, 0) < 0$, $J(u_2, 0) > 0$ and $J(-N/2M, 0) = 0$ which implies that Q_1 (Q_2) is a saddle (centre) while Q_3 is a cusp point.

For a fixed $M > 0$, from $\Delta = N^2 - 4MG = 0$, one can find the bifurcation curve

$$L_1^{\pm}\colon\ G = G(N) = \frac{N^2}{4M}, \quad N > 0\ (<0).$$

$L_1^{\pm}$ and another bifurcation curve L_2: $G = 0$ divide the (N, G)-parameter plane into different subregions as follows:

$$D_1 = \{(N, G)\,|\,0 < G < G(N),\ N > 0\},$$
$$D_2 = \{(N, G)\,|\,G > G(N),\ N \in \mathbb{R}\},$$
$$D_3 = \{(N, G)\,|\,0 < G < G(N),\ N < 0\},$$
$$D_4 = \{(N, G)\,|\,G < 0,\ N \in \mathbb{R}\}.$$

The phase portraits of (26) are shown in figure 3.

3.2 *The exact travelling wave solutions of eq.* (5) *when* $G \neq 0$

Now we study the exact travelling wave solutions of the mGVE (1). Denote that $h_i^* = H(u_i, 0)\,(i = 1, 2, 3)$ defined by (6), then

$$h_1^* = -\frac{1}{24M^2}(N + \sqrt{\Delta})(8MG - N^2 - N\sqrt{\Delta}),$$
$$h_2^* = -\frac{1}{24M^2}(N - \sqrt{\Delta})(8MG - N^2 + N\sqrt{\Delta}),$$
$$h_3^* = -\frac{N^3}{24M^2}. \quad (28)$$

Similar to §2.2, we obtain the following results:

3.2.1 *Pseudopeakon solution.* For $(N, G) \in D_1$, corresponding to $H(u, y) = h_1^*$ defined by (6), eq. (5) has a homoclinic orbit at the saddle Q_1 shown in figure 3a. As the homoclinic orbit is near the singular line $u = 0$, the corresponding travelling wave solution of (5) forms

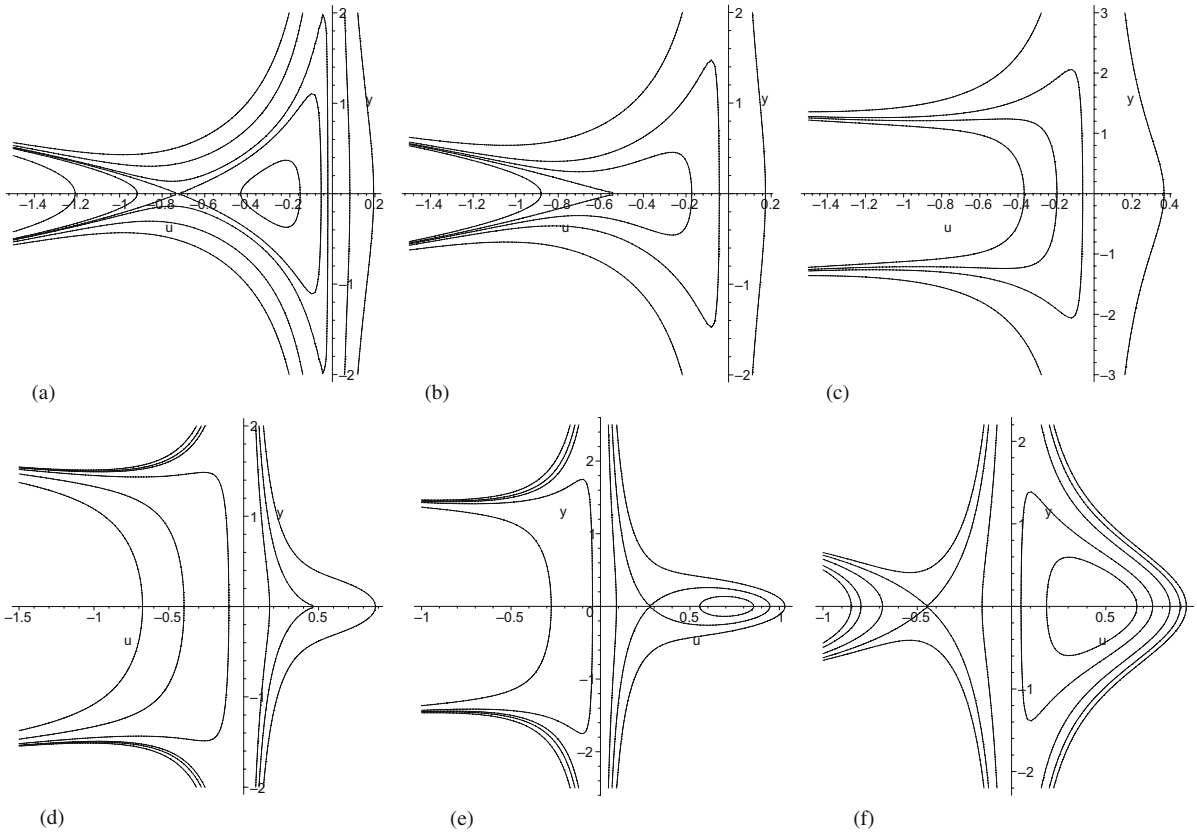

Figure 3. The phase portraits of system (26) for $M > 0$, $G \neq 0$. (**a**) $(N, G) \in D_1$, (**b**) $(N, G) \in L_1^+$, (**c**) $(N, G) \in D_2$, (**d**) $(N, G) \in L_1^-$, (**e**) $(N, G) \in D_3$ and (**f**) $(N, G) \in D_4$.

a profile of pseudopeakon. It follows from $H(u, y) = h_1^*$;in (6) that

$$y = \pm\frac{\sqrt{6M}}{3u}(u - u_1)\sqrt{\phi_m - u}\,, \tag{29}$$

where

$$\phi_m = \frac{N - 2\sqrt{\Delta}}{-2M} < 0.$$

Substituting (29) into the first equation of (5) and integrating it with the initial value $u(0) = \phi_m$ yields

$$\int_u^{\phi_m} \frac{u\,\mathrm{d}u}{(u - u_1)\sqrt{\phi_m - u}} = \pm\int_\xi^0 \sqrt{\frac{2M}{3}}\mathrm{d}\xi. \tag{30}$$

Then one can get the parametric representation of the pseudopeakon solution of (5)

$$\begin{cases} u(\chi) = \phi_m - (\phi_m - u_1)\,\tanh^2(\chi), \\ \xi(\chi) = \sqrt{\dfrac{6}{M}}\left(\sqrt{\phi_m - u_1}\tanh(\chi) + \dfrac{u_1\chi}{\sqrt{\phi_m - u_1}}\right), \end{cases} \tag{31}$$

where $\chi \in \mathbb{R}$ plays the parametric role in these dependences. The plot of the pseudopeakon solution (31) is shown in figure 4a.

3.2.2 *Smooth periodic wave solutions.* As $(N, G) \in D_1 \cup D_3 \cup D_4$, corresponding to $H(u, y) = h \in (h_2^*, h_1^*)$, there exists a family of smooth periodic wave solutions which has the same parametric representations as (25), but in this case, r_1, r_2 and r_3 with $r_1 < r_2 < r_3$ are the three real roots of the equation $2Mu^3 + 3Nu^2 + 6Gu - 6h = 0$.

3.2.3 *Cusped soliton solution.*

Case 1. When $(N, G) \in D_3 \cup D_4$, corresponding to $H(u, y) = h_1^*$, there is a stable manifold and aunstable manifold both of which cross the saddle Q_1 and are close to the singular line $u = 0$ (see figures 3e and 3f). Similar to §3.2.1, substituting (29) into the first equation of eq. (5) and integrating it with the initial

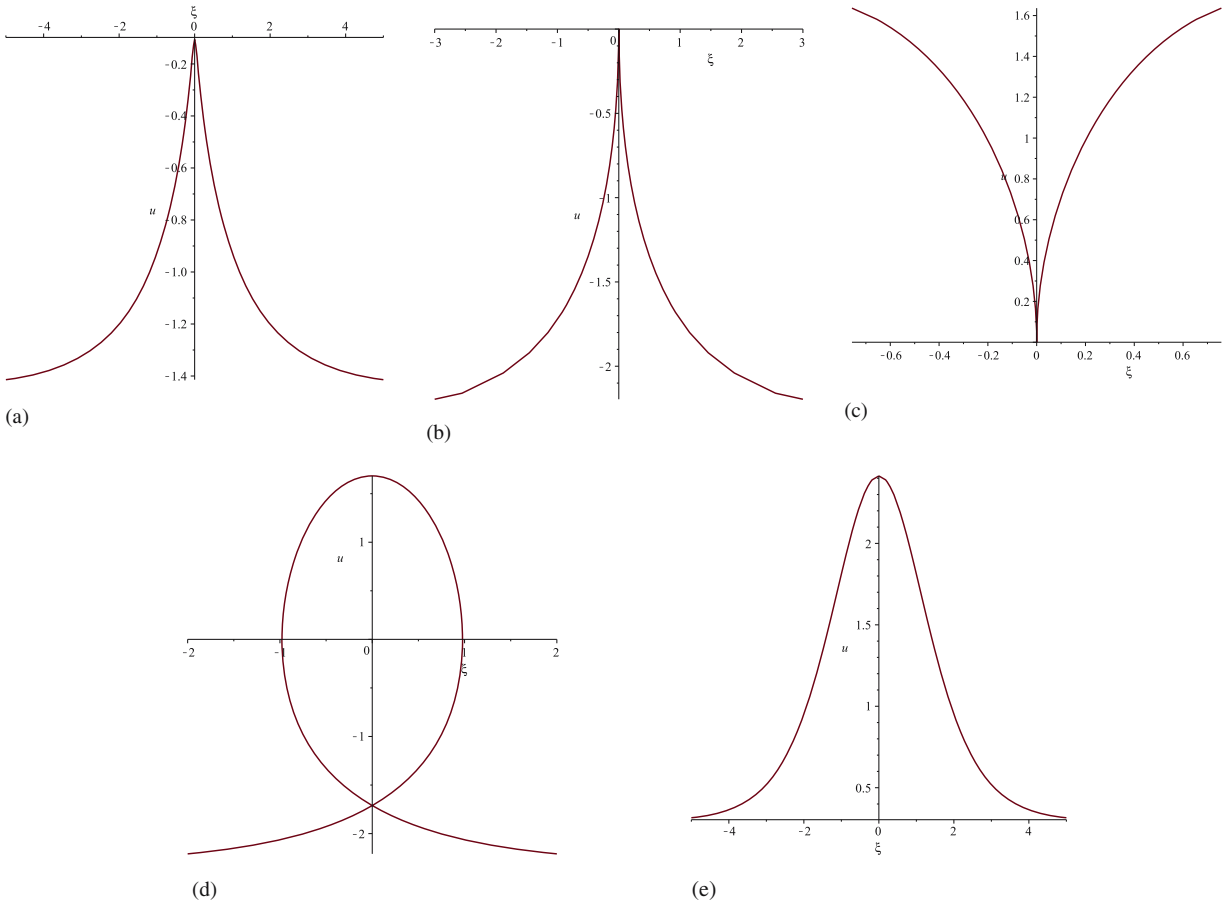

Figure 4. The wave profiles of $u(\xi)$ with different types. (**a**) Pseudopeakon, (**b**) cuspon with peak type, (**c**) cuspon with valley type, (**d**) loop-soliton and (**e**) smooth soliton.

value $u(0) = 0$ yields

$$\int_u^0 \frac{u\,\mathrm{d}u}{(u-u_1)\sqrt{\phi_m - u}} = \pm \int_\xi^0 \sqrt{\frac{2M}{3}}\mathrm{d}\xi. \tag{32}$$

Then one can get the parametric representation of the cusped soliton solution of (5)

$$\begin{cases} u(\chi) = \phi_m - (\phi_m - u_1)\,\tanh^2(\chi), \\ \xi(\chi) = \pm\sqrt{\dfrac{6}{M}}\left(\sqrt{\phi_m - u_1}\,\tanh(\chi) + \dfrac{u_1\chi}{\sqrt{\phi_m - u_1}} - \mu_2\right), \end{cases} \tag{33}$$

where

$$\mu_2 = \sqrt{\phi_m} + \frac{u_1}{\sqrt{\phi_m - u_1}}\,\tanh^{-1}(v_1),$$

$$\chi \in [\tanh^{-1}(v_1), +\infty)$$

and

$$v_1 = \sqrt{\phi_m/(\phi_m - u_1)}.$$

The wave profile of the cusped soliton solution (31) is shown in figures 4b and 4c.

Case 2. When $(N, G) \in L_1^-$, i.e., $G = N^2/4M$, corresponding to $H(u, y) = h_3^*$, there is a stable manifold and an unstable manifold both of which start from the cusp point Q_3 and are close to the singular line $u = 0$ (see figure 3d). For $h = h_3^*$, it follows from (6) that

$$y = \pm\frac{\sqrt{6M}}{3u}\,(\mu_3 - u)\,\sqrt{\mu_3 - u}, \tag{34}$$

where $\mu_3 = -N/2M$. Substituting (34) into the first equation in (5) and integrating it with the initial value $u(0) = 0$ gives

$$\int_0^u \frac{u\,\mathrm{d}u}{(\mu_3 - u)\sqrt{\mu_3 - u}} = \pm \int_0^\xi \sqrt{\frac{2M}{3}}\mathrm{d}\xi. \tag{35}$$

Hence eq. (5) has the following cusped soliton solution with implicit function form:

$$2\sqrt{3}u + 4\sqrt{3\mu_3(\mu_3 - u)} - 4\sqrt{3}\,\mu_3 + \text{sign}(\xi)\sqrt{2M(\mu_3 - u)}\,\xi = 0. \tag{36}$$

3.2.4 *Loop soliton solution.* As $(N, G) \in D_4$, corresponding to $H(u, y) = h_1^*$, similar to §3.2.1, one can obtain the following loop soliton:

$$\begin{cases} u(\chi) = \phi_m - (\phi_m - u_1)\,\tanh^2(\chi), \\ \xi(\chi) = \sqrt{\dfrac{6}{M}}\left(\sqrt{\phi_m - u_1}\tanh(\chi) + \dfrac{u_1\chi}{\sqrt{\phi_m - u_1}}\right). \end{cases} \tag{37}$$

The wave profile of the loop soliton solution (37) is shown in figure 4d.

3.2.5 *Smooth soliton solution.* When $(N, G) \in D_3$, corresponding to $H(u, y) = h_1^*$, there is a smooth and analytic homoclinic orbit at the saddle Q_1 enclosing the centre Q_2, which yields a smooth soliton solution of (5). Similar to §3.2.4 one can obtain the smooth soliton solution with peak type

$$\begin{cases} u(\chi) = \phi_m - (\phi_m - u_1)\,\tanh^2(\chi), \\ \xi(\chi) = \sqrt{\dfrac{6}{M}}\left(\sqrt{\phi_m - u_1}\tanh(\chi) + \dfrac{u_1\chi}{\sqrt{\phi_m - u_1}}\right). \end{cases} \tag{38}$$

With the aid of *Maple*, one can gain the wave profile of the smooth soliton solution (38) shown in figure 4e.

Remark 3. When $(N, G) \in D_1$, there exists a homoclinic orbit given by a branch of the curves $H(u, y) = h_1^*$ and a family of periodic orbits defined by $H(u, y) = h$ for $h \in (h_2^*, h_1^*)$. As h varies from h_2^* to h_1^*, the periodic solutions determined by the above periodic orbits will gradually evolve from non-peaked periodic waves to the smooth periodic cusp-like waves and finally converge to the pseudopeakon determined by the homoclinic orbit.

Remark 4. Although eqs (31), (37) and (38) have the same expressions, they display different dynamical behaviours: pseudopeakon, loop soliton and smooth soliton, respectively. The same formulas have rich dynamical property by taking different parametric values. So it is very important to study the dynamical behaviour of the travelling wave solutions of nonlinear evolution equations.

4. Conclusion

In this paper, we have studied the bifurcations and dynamical behaviour of travelling wave solutions of the modified generalized Vakhnenko equation and obtained many smooth and non-smooth travelling wave solutions such as smooth soliton, smooth periodic wave solutions, pesudopeakon solution, periodic cusped wave solution, cusped soliton solution, loop soliton solution and so on.

Acknowledgements

This research is supported by National Natural Science Foundation of China (Nos 11162004, 11461021), Guangxi Natural Science Foundation (No. 2015GXNS FBA139004) and Innovation Project of GUET Graduate Education (No. YJCXS201557).

References

[1] V A Vakhnenko, *J. Phys. A*: *Math. Gen.* **25**, 4181 (1992)
[2] E J Parkes, *J. Phys. A*: *Math. Gen.* **26**, 6469 (1993)
[3] V O Vakhnenko, *Ukr. J. Phys.* **42**, 104 (1997)
[4] V O Vakhnenko and E J Parkes, *Nonlinearity* **11**, 1457 (1998)
[5] V O Vakhnenko and E J Parkes, *Chaos, Solitons and Fractals* **13**, 1819 (2002)
[6] Y Y Wu, C Wang and S J Liao, *Chaos, Solitons and Fractals* **23**, 1733 (2005)
[7] Y L Ma and B Q Li, *J. Math. Phys.* **51**, 063512 (2010)
[8] V O Vakhnenko, E J Parkes and A J Morrison, *Chaos, Solitons and Fractals* **17**, 683 (2003)
[9] A J Morrison and E J Parkes, *Chaos, Solitons and Fractals* **16**, 13 (2003)
[10] Y L Ma, B Q Li and C Wang, *Appl. Math. Comput.* **211**, 102 (2009)
[11] Y L Ma and B Q Li, *Appl. Math. Comput.* **219**, 2212 (2012)
[12] A M Wazwaz, *Phys. Scr.* **82**, 065006 (2010)
[13] M S Hashemi, M C Nucci and S Abbasbandy, *Commun. Nonlinear Sci. Numer. Simul.* **18**, 867 (2013)
[14] J Guckenherimer and P J Holmes, *Nonlinear oscillations, dynamical systems and bifurcation of vector fields* (Springer-Verlag, New York, 1983)
[15] D H Feng and J B Li, *Pramana – J. Phys.* **68**, 963 (2007)
[16] Y A Xie, S Q Tang and D H Feng, *Pramana – J. Phys.* **78**, 499 (2012)
[17] J B Li and Z J Qiao, *J. Math. Phys.* **54**, 123501 (2013)
[18] L Y Zhong, S Q Tang and L J Qiao, *Nonlinear Dyn.* **80**, 129 (2015)
[19] P F Byrd and M D Friedman, *Handbook of elliptic integrals for engineers and physicists* (Springer-Verlag, Berlin, 1954)